Numerical Study of Hydrogen–Air Detonation in Vibrational Non-equilibrium

L. S. Shi, P. Zhang, C. Y. Wen, H. Shen, M. Parsani, and D. L. Zhang

Abstract The effects of vibrational non-equilibrium and vibration–chemistry coupling on hydrogen–air detonation are numerically investigated by solving reactive Euler equations coupled with a multiple vibrational temperature-based model. Detailed hydrogen–air reaction kinetic is utilized, Landau–Teller model is adopted to solve the vibrational relaxation process, and the coupled vibration–chemistry vibration model is used to evaluate the vibration–chemistry coupling. It is shown that the relaxation process and vibration–chemistry coupling considerably influence the hydrogen–air detonation structure, highlighting the importance of correct treatment of vibrational non-equilibrium in detonation simulations.

1 Introduction

The complex multiscale physical phenomena in hydrogen detonation have been studied by numerical simulations for some years. These studies have focused on various aspects of detonation: projectile-induced detonation [1], rectangular/diagonal modes in three-dimensional hydrogen–air detonation [2], and the deflagration-to-detonation transition [3]. Due to the intrinsically unsteady and highly nonlinear characteristics of detonation and the unclear mechanism of reactions under extreme conditions, the detailed fundamental characteristics of detonation remain poorly

L. S. Shi · P. Zhang · C. Y. Wen (✉)
Department of Mechanical Engineering, The Hong Kong Polytechnic University, Hung Hom, Hong Kong
e-mail: cywen@polyu.edu.hk

H. Shen · M. Parsani
King Abdullah University of Science and Technology (KAUST), Computer Electrical and Mathematical Science and Engineering Division (CEMSE), Extreme Computing Research Center (ECRC), Thuwal, Saudi Arabia

D. L. Zhang
State Key Laboratory of High Temperature Gas Dynamics, Institute of Mechanics, Chinese Academy of Sciences, Beijing, China

A. Sasoh et al. (eds.), *31st International Symposium on Shock Waves 2*,
https://doi.org/10.1007/978-3-319-91017-8_19

understood. The vibrational degree of freedom in air is relatively slowly equilibrated in high-enthalpy flows [4, 5], and the resulting vibration–chemistry coupling has been widely researched [6, 7]. The time scales of vibrational relaxation are comparable to those of ignition behind the detonation wave [8]. This overlap has necessitated careful investigation with a combination of computational and practical approaches to the physical processes and vibrational relaxation involved.

In this paper, several two-dimensional simulations are performed for a stoichiometric hydrogen–air mixture at 1 atm and 300 K, under the various assumptions of vibrational equilibrium, non-equilibrium, or vibration–chemistry coupling, to understand the underlying physics. The computations are performed using the supercomputer Shaheen XC-40 installed at King Abdullah University of Science and Technology.

2 Methodology

The space–time conservation element and solution element (CE/SE) method [9] is a compact numerical scheme in which only the information of the neighboring mesh points is required for each time step, making it ideal for large-scale computing. This method has been developed [10–12], implemented, and validated in several studies of variable complex flows, including compressible multicomponent flows [13] and gaseous detonations [14, 15]. In this study, the CE/SE method was extended to solve the two-dimensional unsteady reactive Euler equation:

$$\frac{\partial \mathbf{U}}{\partial t} + \frac{\partial \mathbf{F}}{\partial x} + \frac{\partial \mathbf{G}}{\partial y} = \mathbf{S} \tag{1}$$

where $\mathbf{U}$ is the conserved vector, consisting of the individual species densities, ρ_i; the momentums, ρu and ρv; the total energy, E; and the vibrational energies of the different molecular species, $\rho_i e_{\mathrm{v,i}}$:

$$\mathbf{U} = \left[\rho_1, \cdots, \rho_{\mathrm{Ns}}, \rho u, \rho v, E, \rho_i e_{\mathrm{v},1}, \cdots, \rho_{\mathrm{Nm}} e_{\mathrm{v,Nm}}\right] \tag{2}$$

with $\mathrm{N_S}$ the number of species and $\mathrm{N_m}$ the number of molecular species. $\mathbf{F}$ and $\mathbf{G}$ are the corresponding fluxes in the x and y directions, respectively.

It was assumed that the vibrational energy was decoupled from the translational–rotational energy. The total energy E comprises the energy in the translational–rotational mode, enthalpy of formation, vibrational energy, and flow kinetic energy:

$$E = \sum_{i=1}^{\mathrm{Ns}} \rho_i C_{v,\mathrm{tr},i} T_{\mathrm{tr}} + \sum_{i=1}^{\mathrm{Ns}} \rho_i h_i^0 + \sum_{\text{molecule}} \rho_i e_{\mathrm{v},i}\left(T_{\mathrm{v},i}\right) + \frac{1}{2}\rho\left(u^2 + v^2\right) \tag{3}$$

The vibrational energy of molecule i is expressed as a function of the species gas constant, vibrational temperature $T_{\mathrm{v},i}$, and characteristic vibrational temperature θ_i:

$$e_{\mathrm{v},i}\left(T_{\mathrm{v},i}\right) = R_i \frac{\theta_i}{e^{\theta_i / T_{\mathrm{v},i}} - 1} \tag{4}$$

S is the source term that represents the chemical reactions and energy exchange between translational–rotational energy and individual vibrational energies. The chemical reactions were modeled by the mechanisms for high-pressure high-temperature hydrogen combustion [16], which include nine species (H_2, O_2, H, O, OH, HO_2, H_2O, H_2O_2, and N_2) and 23 reactions. Nitrogen was modeled as an inert diluent. The calculation of chemical reaction rates according to the CHEMKIN manual [17] was embedded in the codes. The ignition delay times calculated in this work agreed well with the data from Burke et al. [16].

The interspecies vibrational relaxation times were calculated using Millikan and White's formulation [18], and the vibrational energy relaxation rates were calculated using the Landau–Teller model [19]:

$$S_{\mathrm{tr-v},i} = \rho_i \frac{e_{\mathrm{v},i}\left(T_{\mathrm{tr}}\right) - e_{\mathrm{v},i}\left(T_{\mathrm{v},i}\right)}{\tau_i} \tag{5}$$

The physically consistent coupled vibration–chemistry vibration (CVCV) model [6] was applied to evaluate the effect of vibrational non-equilibrium on the reaction rates. In this model, the chemical reaction rate is modified by an efficiency function, $\varphi(T_{\mathrm{tr}}, T_{\mathrm{v}}) = k(T_{\mathrm{tr}}, T_{\mathrm{v}}) / k^E(T_{\mathrm{tr}})$:

$$\varphi\left(T_{\mathrm{tr}}, T_{\mathrm{v}}\right) = \frac{Q\left(T_{\mathrm{tr}}, E_{\mathrm{d}}\right)}{Q\left(T_{\mathrm{tr}}, E_{\mathrm{d}}\right)} \cdot \frac{e^{-\frac{\alpha E_{\mathrm{a}}}{RT}} Q\left(\Gamma, \alpha E_{\mathrm{a}}\right) + Q\left(T^0, E_{\mathrm{d}}\right) - Q\left(T^0, \alpha E_{\mathrm{a}}\right)}{e^{-\frac{\alpha E_{\mathrm{a}}}{RT}} Q\left(-U, \alpha E_{\mathrm{a}}\right) + Q\left(T^*, E_{\mathrm{d}}\right) - Q\left(T^*, \alpha E_{\mathrm{a}}\right)} \tag{6}$$

where $1/\Gamma = 1/T_{\mathrm{v}} - 1/T_{\mathrm{tr}} - 1/U$, $1/T^0 = 1/T_{\mathrm{v}} - 1/U$, and $1/T^* = 1/T_{\mathrm{tr}} - 1/U$ with coefficient $\alpha = 0.8$, $U = E_{\mathrm{d}}/5R$, and $Q(T, E) = [1 - \exp(-E/RT)]/[1 - \exp(-\theta_{\mathrm{v}}/T)]$.

3 Results

The computational domain was filled with a stoichiometric hydrogen−air mixture with initial conditions of $P_0 = 1$ atm and $T_0 = 300$ K. The left, upper, and lower sides of the computational domain were treated with slip-wall boundary conditions. A narrow area with $T_s = 4000$ K and $P_s = 90$ atm was used to ignite the mixture, and small energy perturbations were added in this hot region to trigger the instabilities. In the simulations, variations in the form or size of the perturbations were found to exert a negligible influence on the final cellular sizes and regularities provided

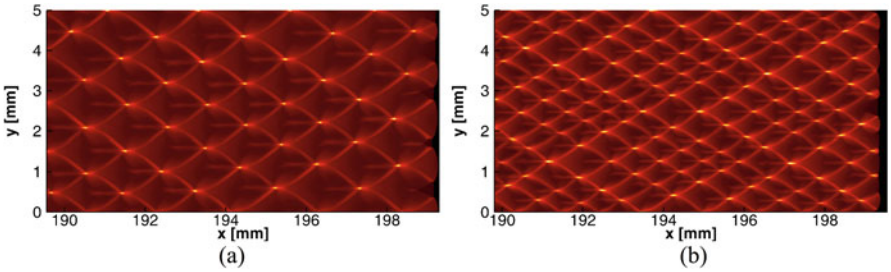

Fig. 1 (**a**) Detonation cellular pattern under assumption of thermodynamic equilibrium. (**b**) Detonation cellular pattern with finite transfer rate of molecular translational–rotational energy to vibrational energy

that the detonation waves were long enough. Three cases were considered: (1) the vibrational modes were assumed to be equilibrated with the translational–rotational modes; (2) the vibrational modes were assumed to be frozen across the shock wave and then relax to equilibrium via the Millikan–White relation; and (3) based on the second case, the chemical mechanisms were manipulated by the CVCV model [6].

3.1 Influence of Vibrational Relaxation

For the thermal equilibrium case, after the shock wave propagated a relatively long distance (more than 100 cell lengths), it was observed that the cellular structures tended to become stable (Fig. 1a). The average cell width was around 1.11 mm.

However, in the simulation featuring (uncoupled) vibrational relaxation, the distribution of the cell widths was slightly irregular. Most of the cells shrank to between 0.5 and 0.8 mm, with an average value of 0.63 mm (Fig. 1b). The effect of temperature on the rate of the reaction $H + O_2 = OH + O$ was significant [20]. In this simulation, the initial conditions included a dense mixture of H_2, O_2, and N_2 molecules, and their vibrational temperatures were frozen across the shock wave. This elevated the post-shock translational–rotational temperature, because the vibrationally frozen condition allowed additional energy to be stored in the form of translational–rotational modes [21]. The elevated translational–rotational temperature further accelerated the reactions and resulted in smaller cells. The difference between the first two assumptions was more significant than that reported in H_2-O_2-Ar detonation [15], despite the different initial conditions and reaction kinetics used. This difference may have arisen from the diluent species: the vibrational relaxation process in our system, with the molecular diluent nitrogen (of which the molar fraction in the current simulation was 55.6%), is more complex than that with the atomic diluent argon (of which the molar fraction in Shi et al. [15] was 70%).

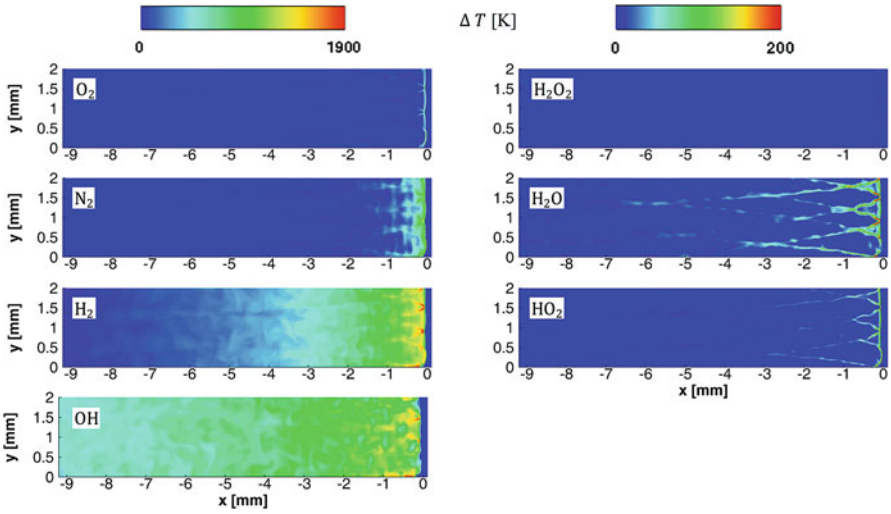

Fig. 2 Differences between translational–rotational temperature and species vibrational temperature ($T_{\mathrm{tr}} - T_{\mathrm{v},i}$) near the bottom region of the computational domain in Fig. 1b

3.2 Influence of Vibration–Chemical Coupling

After the shock passed through the mixture, O_2 approached thermal equilibrium most quickly, whereas the vibrational temperature of N_2 increased more gradually, and it took much longer distance before H_2 reached thermal equilibrium (see Fig. 2).

The effect of the ignition delay time on the reaction-zone structure was considerable. In typical post-shock conditions of hydrogen–air detonation, the sensitivity analysis for individual reaction rates revealed that the ignition delay time was most sensitive to the chain branching reaction $\mathrm{H} + \mathrm{O_2} = \mathrm{O} + \mathrm{OH}$. When evaluating the effect of vibration–chemistry coupling using the CVCV model, the reaction rates were multiplied by an efficiency factor, which was a function of translational–rotational temperature and species vibrational temperature. From Fig. 3, it can be observed that even a very small difference between the vibrational temperature and the translational–rotational temperature suppressed the reaction rate significantly.

Because there was a region in which individual vibrational temperatures deviated from the translational temperature, the cellular structure in the third case was significantly affected by the vibration–chemistry coupling (Fig. 4); the cellular structure was found to be irregular, with average cell widths of roughly 3.33 mm across the simulation domain.

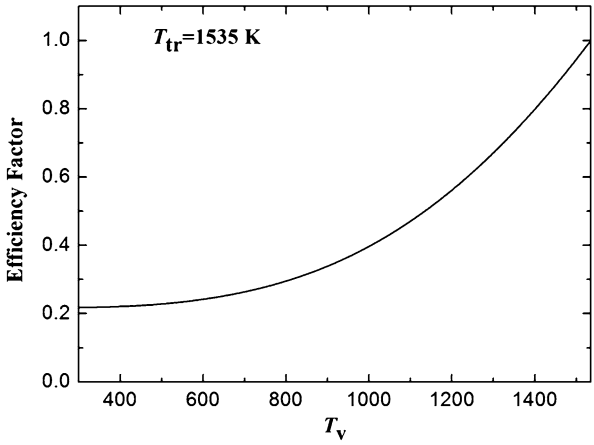

Fig. 3 Efficiency factor for reaction $H + O_2 \rightarrow O + OH$, with the translational–rotational temperature fixed at 1535 K

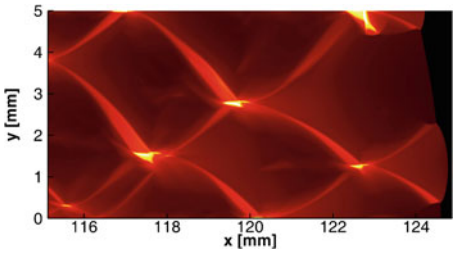

Fig. 4 Detonation cellular pattern using CVCV model

4 Conclusion

Time-dependent numerical simulations were performed using a detailed reaction model to evaluate the effect of vibrational non-equilibrium on the unstable hydrogen–air detonation, in which the vibrational equilibrium was evaluated for each individual species. The analyses indicated that under post-shock conditions, the reaction most sensitive to the ignition delay time was the chain branching reaction $H + O_2 = O + OH$. When the vibration–chemistry coupling was considered, the reaction rates were greatly suppressed in the non-equilibrium region. Compared with the vibration–chemistry coupling case, our results imply that a numerical simulation that failed to account for the vibrational relaxation process and its coupling with the chemistry would be likely to underestimate the detonation cell size.

Acknowledgment We are grateful for the computing resources of the Supercomputing Laboratory and the Extreme Computing Research Center at King Abdullah University of Science and Technology. This research was supported by Hong Kong Innovation and Technology Commission (no. ITS/334/15FP) and Natural Science Foundation of China project, numbered 11372265.

References

1. M.J. Kaneshige, *Gaseous Detonation Initiation and Stabilization by Hypervelocity Projectiles* (California Institute of Technology, Pasadena, 1999)
2. N. Tsuboi et al., Three-dimensional numerical simulation for hydrogen/air detonation: Rectangular and diagonal structures. Proc. Combust. Inst. **29**, 2 (2002)
3. V.N. Gamezo et al., Numerical simulations of flame propagation and DDT in obstructed channels filled with hydrogen–air mixture. Proc. Combust. Inst. **31**, 2 (2007)
4. R. Millikan, D. White, Vibrational relaxation in air. AIAA J. **2**, 10 (1964)
5. V. Komarov, Role of vibrational relaxation in the nonequilibrium flow of air in nozzles. J. Appl. Mech. Tech. Phys. **19**, 2 (1978)
6. O. Knab et al., Theory and validation of the physically consistent coupled vibration-chemistry-vibration model. J. Thermophys. Heat Transf. **9**, 2 (1995)
7. C. Park, Assessment of a two-temperature kinetic model for dissociating and weakly ionizing nitrogen. J. Thermophys. Heat Transf. **2**, 1 (1988)
8. B. Taylor et al., Estimates of vibrational nonequilibrium time scales in hydrogen-air detonation waves, in *24th International Colloquium on the Dynamics of Explosive and Reactive Systems*, Taipei, Taiwan, July 2013
9. S.-C. Chang, The method of space-time conservation element and solution element—A new approach for solving the Navier-Stokes and Euler equations. J. Comput. Phys. **119**, 2 (1995)
10. H. Shen, C.-Y. Wen, A characteristic space–time conservation element and solution element method for conservation laws II. Multidimensional extension. J. Comput. Phys. **305**, 775–792 (2016)
11. H. Shen et al., Robust high-order space–time conservative schemes for solving conservation laws on hybrid meshes. J. Comput. Phys. **281**, 375–402 (2015)
12. H. Shen et al., A characteristic space–time conservation element and solution element method for conservation laws. J. Comput. Phys. **288**, 101–118 (2015)
13. H. Shen et al., Maximum-principle-satisfying space-time conservation element and solution element scheme applied to compressible multifluids. J. Comput. Phys. **330**, 668–692 (2017)
14. H. Shen, M. Parsani, The role of multidimensional instabilities in direct initiation of gaseous detonations in free space. J. Fluid Mech. **813**, R4 (2017)
15. L. Shi et al., Assessment of vibrational non-equilibrium effect on detonation cell size. Combust. Sci. Technol. **189**, 5 (2016)
16. M.P. Burke et al., Comprehensive H2/O2 kinetic model for high-pressure combustion. Int. J. Chem. Kinet. **44**, 7 (2012)
17. R.J. Kee et al., *CHEMKIN-III: A FORTRAN chemical kinetics package for the analysis of gas-phase chemical and plasma kinetics*, Sandia national laboratories report SAND96-8216 (1996)
18. R.C. Millikan, D.R. White, Systematics of vibrational relaxation. J. Chem. Phys. **39**, 12 (1963)
19. W.G. Vincenti, C.H. Kruger, *Introduction to Physical Gas Dynamics* (Krieger, Malabar, 1965), pp. 198–206
20. Z. Hong et al., A new shock tube study of the H + O 2 → OH + O reaction rate using tunable diode laser absorption of H 2 O near 2.5 μm. Proc. Combust. Inst. **33**, 1 (2011)
21. M.F. Campbell et al., Dependence of calculated postshock thermodynamic variables on vibrational equilibrium and input uncertainty. J. Thermophys. Heat Transf. **31**, 586–608 (2017)